UCRL- 96361
PREPRINT

METALLURGICAL EFFECTS ON THE CONSTITUTIVE AND FRAGMENTATION BEHAVIOR OF OFHC COPPER RINGS

W. H. Gourdin

This paper was prepared for submittal to
Proceedings of the APS 1987 Topical Conference
on Shock waves in Condensed Matter,
Monterey, California, 20-23 July, 1987

July 7, 1987

Lawrence Livermore National Laboratory

METALLURGICAL EFFECTS ON THE CONSTITUTIVE AND FRAGMENTATION BEHAVIOR OF OFHC COPPER RINGS

W. H. Gourdin

Lawrence Livermore National Laboratory, P.O. Box 808, Livermore, CA 94550

I report preliminary results of recent constitutive and fragmentation studies on electromagnetically launched expanding ring specimens of fully annealed OFHC copper with grain sizes of 10, 30-50, 90-120, and 150-200 μm. Grain size correlations with material behavior are developed and briefly discussed in reference to previous data, with particular attention to thermodynamic models of fragmentation.

1. INTRODUCTION

Although the expanding ring has been applied to the study of both the fragmentation[1-3] and the constitutive[4-8] properties of metals at tensile strain rates of the order of $10^4\ s^{-1}$, there has apparently been no systematic study of the effects of initial metallurgical condition on either of these phenomena using this technique. Here I will briefly describe some preliminary results of studies of grain size effects on the material behavior observed in expanding ring specimens of OFHC copper (alloy 101) with grain sizes of 10, 30-50, 90-120 and 150-200 μm. I will first describe the specimen characteristics and preparation, then outline our experiments and diagnostics. A presentation of preliminary results for a limited number of experiments follows, together with comparisons with previous data. I will conclude with a discussion of our data in the context of recent models of ring fragmentation.[3]

2. EXPERIMENTAL

2.1 Specimen preparation

The material used in this study was stock OFHC copper obtained in the form of hot-rolled plate, 5 cm thick. Cubes 5 cm on a side were compressed 75% along each orthogonal axis in increments of 25%, applied sequentially. This treatment introduced a considerable amount of work without the development of strong textures. Various heat-treatment schedules (Table 1) were then employed to achieve the final grain sizes. Note that the 90-120 μm material required intermediate working. The hardness shows the expected decrease with increasing grain size, but otherwise indicates that all the materials are in a fully soft condition. Grain sizes were determined by comparison with ASTM standard plates for twinned grains.

2.2 Experiments

The experimental apparatus is described in detail in references 9 and 10. We use the electromagnetic launch method[9,10] to avoid shock wave effects,[7,11] and material stresses are inferred from the deceleration of the ring as measured with a velocity interferometer (VISAR). The fragmentation of the specimen is recorded with a framing camera, and all fragments are collected and examined. Specimen and solenoid currents, measured with Rogowski probes, are

TABLE 1
Heat-treatment schedule and hardness of starting materials worked 75% along each orthogonal axis.

Final grain size (μm)	Heat treatment schedule	Hardness (kg/mm^2)
10	10 min at 300°C, in flowing argon sand bath	60
30-50	30 min at 500°C, in flowing argon sand bath	53
90-120	30 min at 500°C, flowing argon sand bath; 20% cold roll; 30 min at 800°C in vacuum	--
150-200	60 min at 800°C in vacuum	45

used to infer the average temperature rise from Joule heating, about 150°C.[10]

3. RESULTS

3.1 Constitutive behavior

The stress-strain behavior for several specimens of 10-μm-grain-size material is shown in Fig. 1. These data were smoothed using digital filtering methods and Fourier analysis. All the curves appear to approach the same ultimate stress, about 380 MPa. The strain rate as a function of strain is shown in Fig. 2, from

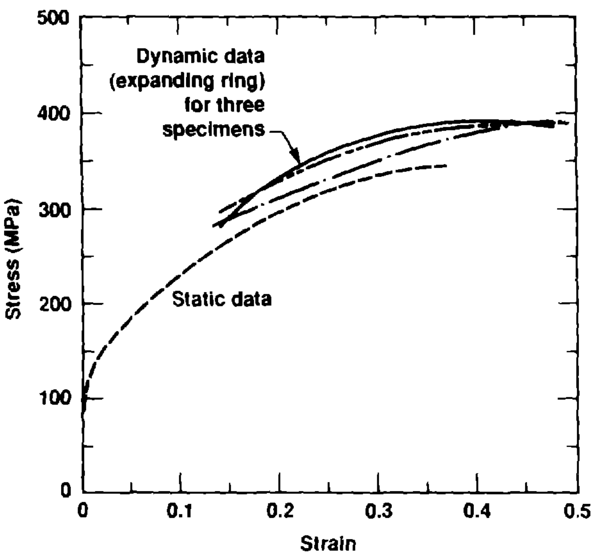

FIGURE 1
Dynamic stress-strain data for 10 μm material (i.e., grain size is 10 μm).

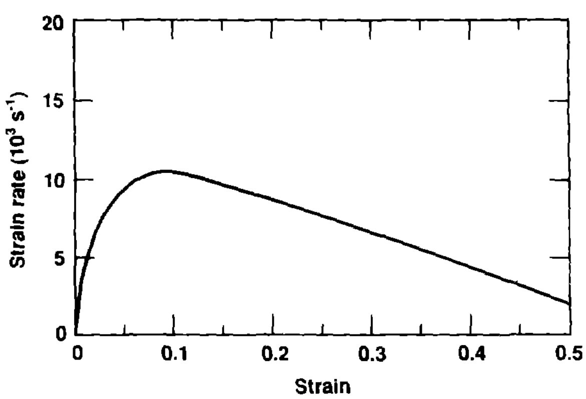

FIGURE 2
Strain rate as a function of strain.

which it is apparent that, although the peak strain rate is about 10^4 s^{-1}, much of the data of Fig. 1 occurs at rates of 2-8 x 10^3 s^{-1}. Static data, obtained for rolled material of the same grain size, is also shown in Fig. 1; it falls 20-50 MPa below the dynamic data, in reasonable accord with previous observations in the same strain and strain-rate ranges.[12] The stress-strain relationships obtained for 150-200 μm material (Fig. 3) show a spread similar to that of the 10 μm material in Fig. 1, and all of the curves rise to about 320 MPa at failure. Representative data for 150-200 μm specimens consistently fall 20-60 MPa below data for 10 μm specimens, in contrast to the crossover reported for static tests on copper.[13] Note that the large grain size of the 150-200 μm material relative to the specimen cross section (0.1 cm) may affect these results.

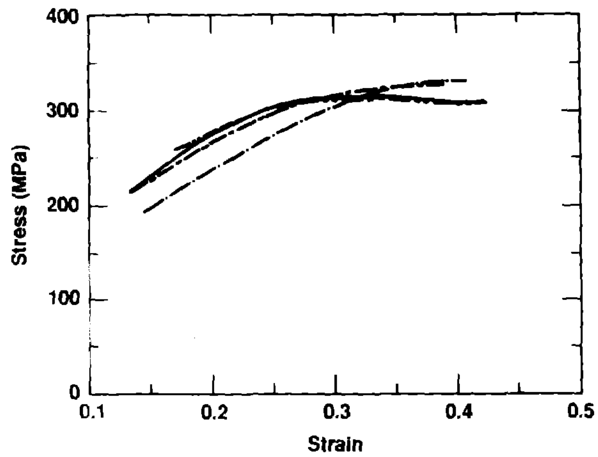

FIGURE 3
Dynamic stress-strain data for 150-200 μm material.

3.2 Fragmentation

The fragmentation data for fixed expansion conditions are summarized in Table 2, and the number of fragments, N, normalized to the relative ring circumference at failure, r/r_0, versus the strain rate at failure is shown in the ln-ln plot in Fig. 4. The failure strain and number of fragments correlate with grain size, although the number of fragments is virtually the same for both of the larger grain sizes. Figure 4 shows that, for constant failure strain-rate, increasing the grain size reduces the average number of fragments. Considering the 20-fold range of grain size, this effect is small. Because all of the specimens experience a similar expansion-speed history, however, the decreasing failure strain implies an increasing strain rate at failure as the grain size increases. Hence there is an implicit grain size effect through the strain rate at failure. Apparently the strain at which plastic instabilities occur decreases as grain size increases. The number

TABLE 2
Summary of fragmentation data. Ranges are 95% confidence intervals. All experiments done at 4 kV.

	Grain size (μm)			
	10	30-50	90-120	150-200
Number of fragments	6.5±2.6	7.5±3.0	9.1±3.0	9.2±2.4
Failure strain	0.49±0.04	0.47±0.04	0.44±0.09	0.40±0.06
Instabilities	14.7±5.2	14.0±6.2	15.7±5.8	16.4±4.8
Number of experiments	22	22	20	20

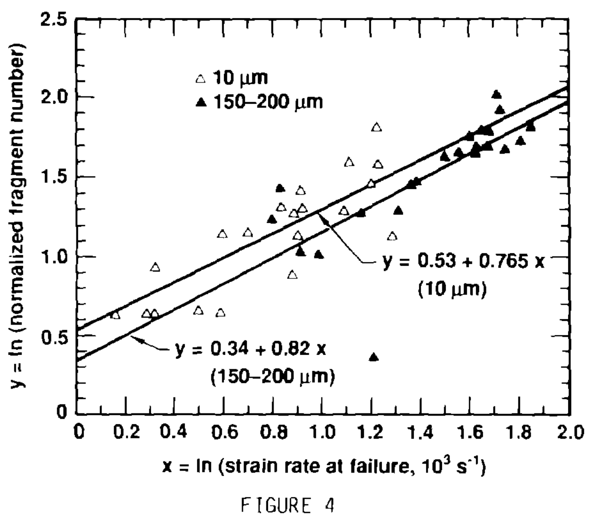

FIGURE 4
Plot (ln-ln) of the normalized number of fragments versus the strain rate at failure. Lines are least-squares fits to the data.

of instabilities (fragments + arrested necks) does not vary strongly with grain size, suggesting that random physical imperfections common to all specimens serve as nuclei for failure.

4. DISCUSSION

By ignoring ring curvature and equating the kinetic energy relative to the center of mass of a stretching fragment with the energy required for a fracture, γ, an expression for the mean fragment length,

$$d = \left(\frac{24\gamma}{\rho}\right)^{1/3} \dot{\varepsilon}^{-2/3}, \quad (1)$$

can be obtained,[3] where ρ is the density and $\dot{\varepsilon}$ is the strain rate. Noting that the relative circumference at failure is

$$L = 2\pi r_0 \exp(\varepsilon_f), \quad (2)$$

where r_0 is the initial mean radius of the specimen and ε_f is the strain at failure, then we see that the number of fragments, N = L/d, can be expressed as

$$\ln(N) - \varepsilon_f = \ln\left[2\pi r_0 \left(\frac{\rho}{24\gamma}\right)^{1/3}\right] + \frac{2}{3} \ln \dot{\varepsilon}. \quad (3)$$

The expression on the left is just the normalized number of fragments, and we thus expect the slope in Fig. 4 to be 2/3. A least-squares analysis gives somewhat larger slopes of 0.76-0.82. Properly accounting for the ring curvature (Eq. (1) is strictly valid only for $d/r \ll 1$) and the presence of unbroken necks will reduce the observed slopes. Note that in the context of Eq. (1), the grain size dependence of the number of fragments obtained at constant strain rate may be attributed to changes in the fracture energy, γ.

5. CONCLUSIONS

From the results presented here, I draw the following preliminary conclusions:

1. Constitutive data obtained from VISAR measurements on electromagnetically launched expanding rings are in qualitative accord with data obtained using other methods.

2. The stresses and strains at failure decrease with increasing grain size, from 380 MPa and 0.5 at a strain rate of about 2.5×10^3 s^{-1} for 10 μm material to 320 MPa and 0.4 at a strain rate of about 5×10^3 s^{-1} for 150-200 μm material.

3. The number of fragments varies with grain size, an effect which can be ascribed both to explicit changes in the fracture energy with grain size and implicit changes in the strain rate at failure through the grain size dependence of the constitutive relationship.

ACKNOWLEDGMENTS

I wish to acknowledge the invaluable help of S. L. Weinland, R. M. Boling, and L. Crouch at all stages of this work. The work was done under the auspices of the U.S. Department of Energy by the Lawrence Livermore National Laboratory under contract W-7405-ENG-48.

REFERENCES

1. D. E. Grady and D. A. Benson, Exp. Mech. 23 (1983) 393.

2. D. E. Grady, M. E. Kipp, and D. A. Benson, Energy and statistical effects in the dynamic fragmentation of metal rings, in: Mechanical Properties at High Rates of Strain, 1984, ed. J. Harding (The Institute of Physics, London, 1984) pp. 315-320.

3. M. E. Kipp and D. E. Grady, J. Mech. Phys. Solids 33 (1985) 399.

4. R. H. Warnes, T. A. Duffey, R. R. Karpp, and A. E. Carden, An improved technique for determining dynamic material properties using the expanding ring, in: Shock Waves and High-Strain-Rate Phenomena in Metals: Concepts and Applications, eds. M. A. Meyers and L. E. Murr (Plenum, New York, 1981) pp. 23-36.

5. A. E. Carden, P. E. Williams, and R. R. Karpp, Comparison of the flow curves of 6061 aluminum alloy at high and low strain rates, ibid. pp. 37-50.

6. T. A. Duffey, R. R. Karpp, R. H. Warnes, J. D. Jacobson, and A. E. Carden, Exp. Tech. 5 (1981) 4.

7. R. H. Warnes, R. R. Karpp, and P. S. Follansbee, J. de Physique Colloque C5, Supplement au no. 8, 46 (1985) C5-583.

8. I. Bransky, M. Hayek, D. Halevy, S. Miller, and Y. Kivity, Determination of dynamic mechanical properties from explosively driven rings, in: Shock Waves in Condensed Matter, ed. Y. M. Gupta (Plenum, New York, 1986) pp. 389-393.

9. W. H. Gourdin, Electromagnetic ring expansion: Experiment, analysis, and application to high-strain-rate testing, in: Proceedings of IMPACT '87, International Conference on Impact Loading and Dynamic Behavior of Materials, Bremen, FRG, May 18-21, 1987, in print.

10. W. H. Gourdin, S. L. Weinland, and R. M. Boling, Electromagnetic ring expansion as a high-rate test: Experimental development, this volume.

11. J. E. Reaugh, Computer simulation and analysis of the expanding ring test, in: Shock Waves in Condensed Matter, ed. Y. M. Gupta (Plenum, New York, 1986) pp. 395-399.

12. P. S. Follansbee, High-strain-rate deformation of FCC metals and alloys, in: Metallurgical Applications of Shock-Wave and High-Strain-Rate Phenomena, eds. L. E. Murr, K. P. Staudhammer, and M. A. Meyers (Marcel Dekker, New York, 1986) pp. 451-479.

13. A. W. Thompson and M. I. Baskes, Phil. Mag. 28 (1973) 301.